Heterotrimetallic Oxalato-Bridged Re$^{IV}_2$M^{II} Complexes (M = Mn, Co, Ni, Cu): Synthesis, Crystal Structure, and Magnetic Properties

José Martínez-Lillo,[†] Fernado S. Delgado,[‡] Catalina Ruiz-Pérez,*[‡] Francesc Lloret,[†] Miguel Julve,[†] and Juan Faus*[†]

Departamento de Química Inorgánica/Instituto de Ciencia Molecular, Facultad de Química de la Universidad de Valencia, Dr. Moliner 50, 46100 Burjassot, Valencia, Spain, and Laboratorio de Rayos X y Materiales Moleculares, Departamento de Física Fundamental II, Universidad de la Laguna, 38204 La Laguna, Tenerife, Spain

The use of the (NBu$_4$)$_2$[Re^{IV}Cl$_4$(ox)] mononuclear species as a ligand toward divalent first row transition metal ions in the presence of imidazole affords the new trinuclear compounds of formula (NBu$_4$)$_2$[{Re^{IV}Cl$_4$(μ-ox)}$_2$M^{II}(Him)$_2$] [NBu$_4^+$ = tetra-*n*-butylammonium cation, ox = oxalate dianion, Him = imidazole; M = Mn (**1**), Co (**2**), Ni (**3**), Cu (**4**)] whose preparation, crystal structures, and magnetic properties are reported. **1**–**4** are isostructural complexes which are made up of discrete trinuclear [{Re^{IV}Cl$_4$(μ-ox)}$_2$M^{II}(Him)$_2$]$^{2-}$ anions and bulky NBu$_4^+$ cations. The Re and M atoms exhibit somewhat distorted octahedral surroundings which are built by four chloro and two oxalate oxygens (Re) and two imidazole nitrogen and four oxalate oxygen atoms (M), the central M atom being linked to the two peripheral Re atoms through bis-bidentate oxalate. The values of the Re···M separation across bridging oxalate vary in the range 5.646(2) (M = Ni) to 5.794(2) Å (M = Mn). Magnetic susceptibility measurements on polycrystalline samples of **1**–**4** in the temperature range 1.9–300 K show the occurrence of significant intramolecular antiferro- (**1**) and ferromagnetic (**2**–**4**) interactions. The nature and magnitude of the magnetic coupling in **1**–**4** are qualitatively understood through orbital symmetry considerations.

Introduction

We are interested in the synthesis of polynuclear complexes containing Re(IV) and first-row transition metal ions to study their magnetic behavior in relation with their structures. This interest is based on different features: (i) the paucity of magneto—structural studies containing 5d transition metal ions;[1] (ii) the strong anisotropy of the paramagnetic Re(IV) ion (it is a 5d^3 ion whose ground electronic state is a ^{4}A$_{2g}$ term with three unpaired electrons but having a value of the spin—orbit coupling constant ca.

1000 cm^{-1} in the free ion);[2] (iii) the large degree of spin delocalization on the ligands which is found in the Re(IV) species that accounts for the intensity of the magnetic interactions observed between the Re(IV) centers at large distances.[3,4] Having this in mind together with the well-known ability of the oxalate ligand (ox) to mediate magnetic interactions between the paramagnetic centers that it bridges,[1a,5] we prepared the [ReCl$_4$(ox)]$^{2-}$ mononuclear complex and

* To whom correspondence should be addressed: E-mail: juan.faus@ uv.es (J.F.), caruiz@ull.es (C.R.-P.).
† Universidad de Valencia.
‡ Universidad de La Laguna.

(1) (a) Kahn, O. *Molecular Magnetism*; VCH: New York 1993. (b) *Molecular Magnetism: From Molecular Assemblies to the Devices*; Coronado, E., Delhaès, P., Gatteschi, D., Miller, J., Eds.; NATO ASI Series E321; Kluwer: Dordrecht, The Netherlands, 1996. (c) *Supramolecular Engineering of Synthetic Metallic Materials*; Veciana, J., Rovira, C., Amabilino, D. B., Eds.; NATO ASI Series C518; Kluwer: Dordrecht, The Netherlands, 1999. (d) Pilkington, M.; Decurtins, S. In *Comprehensive Coordination Chemistry II*; McCleverty, J. A., Meyer, T. J., Eds.; Elsevier: Amsterdam, 2004; Vol. 7, p 177.

(2) (a) Chiozzone, R.; González, R.; Kremer, C.; De Munno, G.; Cano, J.; Lloret, F.; Julve, M.; Faus, J. *Inorg. Chem.* **1999**, *38*, 4745. (b) Chiozzone, R.; González, R.; Kremer, C.; De Munno, G.; Armentano, D.; Cano, J.; Lloret, F.; Julve, M.; Faus, J. *Inorg. Chem.* **2001**, *40*, 4242. (c) Chiozzone, R.; Cuevas, A.; González, R.; Kremer, C.; Armentano, D.; De Munno, G.; Faus, J. *Inorg. Chim. Acta* **2006**, *359*, 2194.

(3) (a) Reynolds, P. A.; Moubaraki, B.; Murray, K. S.; Cable, J. W.; Englhardt, L. M.; Figgis, B. N. *J. Chem. Soc., Dalton Trans.* **1997**, 263. (b) Reynolds, P. A.; Figgis, B. N.; Martín y Marero, D. *J. Chem. Soc., Dalton Trans.* **1999**, 945.

(4) (a) González, R.; Chiozzone, R.; Kremer, C.; De Munno, G.; Nicolò, F.; Lloret, F.; Julve, M.; Faus, J. *Inorg. Chem.* **2003**, *42*, 2512. (b) González, R.; Chiozzone, R.; Kremer, C.; Guerra, F.; De Munno, G.; Lloret, F.; Julve, M.; Faus, J. *Inorg. Chem.* **2004**, *43*, 3013.

(5) Cano, J.; Alemany, P.; Alvarez, S.; Verdaguer, M.; Ruiz, E. *Chem.—Eur. J.* **1998**, *4*, 476 and references therein.

we carried out subsequent studies concerning its use as a ligand toward either fully solvated or partially blocked metal ions.[2a,b,6,7]

The first magneto−structural studies of bimetallic Cu^{II}-Re^{IV} compounds using the $[ReCl_4(ox)]^{2-}$ unit as a complex ligand showed that the coordination modes of the oxalate ligand of the precursor are very sensitive to the nature of the other terminal ligands in the coordination sphere of the copper(II) ion.[2a,b,8] Indeed, the situation of bis-bidentate coordination of the oxalate with two short bonds at the copper atom (which is the most favorable situation to mediate a strong magnetic interaction between the oxalate-bridged metal ions) has not been observed in the $Cu^{II}Re^{IV}$ family. In this respect, the oxalate group of the $[ReCl_4(ox)]^{2-}$ unit was found to act as monodentate[2a,b,8b] and asymmetric bidentate ligand (with one short and one long Cu−O bond)[2] toward the copper atom. This apparent reluctance of the oxalate group from the $[ReCl_4(ox)]^{2-}$ precursor to adopt the wanted bis-bidentate bridging role was overcome as shown in a recent report dealing with the synthesis and magneto−structural characterization of the compounds of formula $[ReCl_4(ox)M^{II}(dmphen)_2]$ (M = Mn, Fe, Co, and Ni and dmphen = 2,9-dimethyl-1,10-phenanthroline).[6] Intramolecular antiferro- (M = Mn) and ferromagnetic (M = Fe, Co, and Ni) interactions are observed in these series, as expected through orbital symmetry considerations.[9]

To substantiate these features and get deeper insights on these fascinating 5d−3d systems, we prepared a new series of isostructural trinuclear compounds of formula $(NBu_4)_2$-$[\{ReCl_4(\mu\text{-}ox)\}_2M(Him)_2]$ with M = Mn (1), Co (2), Ni (3), and Cu (4), Him = imidazole, and NBu_4^+ = tetra-n-butylammonium cation. Their crystal structures and variable-temperature magnetic properties are the subject of this work.

Experimental Section

Materials. The nitrate salts $M(NO_3)_2 \cdot nH_2O$ [M = Mn (n = 4), Co and Ni (n = 6), and Cu (n = 3)], the imidazole, and the organic solvents acetonitrile (MeCN) and 2-propanol (i-PrOH) were purchased from commercial sources and used as received. The complex $(NBu_4)_2[ReCl_4(ox)]$ was prepared by following the previously reported procedure for the corresponding tetraphenylarsonium salt.[2c]

Synthesis of the Complexes. $(NBu_4)_2[\{ReCl_4(ox)\}_2Mn(Him)_2]$ (1). A solution of 90 mg (0.1 mmol) of $(NBu_4)_2[ReCl_4(ox)]$ in an i-PrOH−MeCN (5:1 v/v, 30 mL) mixture was added to a solution of 12.6 mg (0.05 mmol) of $Mn(NO_3)_2 \cdot 4H_2O$ and 6.8 mg (0.1 mmol) of Him in i-PrOH (25 mL). A small amount of a brown microcrystalline solid was removed from the resulting solution. X-ray-quality crystals of 1 as pale green hexagonal plates were obtained by slow evaporation at room temperature after a few days. They were washed with a small volume of cold i-PrOH and diethyl ether. Yield: ca. 60%. Anal. Calcd for $C_{42}H_{80}N_6Cl_8O_8MnRe_2$ (1):

(6) Chiozzone, R.; González, R.; Kremer, C.; De Munno, G.; Armentano, D.; Lloret, F.; Julve, M.; Faus, J. *Inorg. Chem.* **2003**, *42*, 1064.
(7) Martínez-Lillo, J.; Armentano, D.; De Munno, G.; Wernsdorfer, W.; Julve, M.; Lloret, F.; Faus, J. *J. Am. Chem. Soc.* **2006**, *128*, 14218.
(8) (a) Tomkiewicz, A.; Mrozinski, J.; Korybut-Daszkiewcz, B.; Brüdgam, I.; Hartl, H. *Inorg. Chim. Acta* **2005**, *358*, 2135. (b) Tomkiewicz, A.; Mrozinski, J.; Brüdgam, I.; Hartl, H. *Eur. J. Inorg. Chem.* **2005**, 1787.
(9) Pei, Y.; Journaux, Y.; Kahn, O. *Inorg. Chem.* **1983**, *22*, 2624.

C, 33.45; H, 5.35; N, 5.57. Found: C, 33.17; H, 5.40; N, 5.28. IR/cm^{-1}: peaks associated with the oxalate ligand appear at 1697 vs, 1667 vs, and 806 s.

$(NBu_4)_2[\{ReCl_4(ox)\}_2Co(Him)_2]$ (2). The preparation of complex 2 is analogous to that of 1 but using cobalt(II) nitrate hexahydrate instead of the manganese salt and working under an argon atmosphere. A small amount of a pink polycrystalline solid appeared in the closed flask containing the resulting solution after a few days on standing at room temperature. It was filtered off and removed. Then, single crystals of 2 as pink hexagonal plates were separated from the mother liquor by slow evaporation under argon after 1 week. They were washed with small portions of cold i-PrOH and diethyl ether. Yield: ca. 70%. Anal. Calcd for $C_{42}H_{80}N_6$-$Cl_8O_8CoRe_2$ (2): C, 33.36; H, 5.33; N, 5.56. Found: C, 33.27; H, 5.68; N, 5.43. IR/cm^{-1}: peaks associated with the oxalate ligand appear at 1695 vs, 1665 vs, and 808 s.

$(NBu_4)_2[\{ReCl_4(ox)\}_2Ni(Him)_2]$ (3). This complex was prepared by using the same procedure described for 1 but replacing the manganese(II) nitrate by the corresponding nickel(II) salt. As in 1 and 2, the small amount of first obtained solid was filtered off and removed. X-ray-quality crystals of 3, as pale green hexagonal plates, were formed from the mother liquor on standing by slow evaporation at room temperature after 1 week. Yield: ca. 75%. Anal. Calcd for $C_{42}H_{80}N_6Cl_8O_8NiRe_2$ (3): C, 33.37; H, 5.33; N, 5.56. Found: C, 33.34; H, 5.27; N, 5.65. IR/cm^{-1}: peaks associated with the oxalate ligand appear at 1695 vs, 1660 vs, and 810 s.

$(NBu_4)_2[\{ReCl_4(ox)\}_2Cu(Him)_2]$ (4). This complex was prepared through the same procedure described for 1 but using copper(II) nitrate trihydrate (13.2 mg, 0.05 mmol) instead of the manganese salt. A small amount of a green microcrystalline solid was separated from the mother liquor on standing at room temperature after a few days. It was filtered and removed. By further evaporation under ambient conditions green polyhedral crystals of 4 were grown. Yield: ca. 70%. Best crystals of 4 were obtained by performing the synthesis with a 1:1 rhenium to copper molar ratio. Anal. Calcd for $C_{42}H_{80}N_6Cl_8O_8CuRe_2$ (4): C, 33.26; H, 5.32; N, 5.54. Found: C, 32.99; H, 5.53; N, 5.52. IR/cm^{-1}: peaks associated with the oxalate ligand appear at 1699 vs, 1667 vs, and 806 s.

Physical Techniques. The IR spectra were recorded with a Nicolet-Avatar 320 FTIR spectrophotometer as KBr pellets in the $4000-400$ cm^{-1} region. The magnetic measurements on polycrystalline samples of 1−4 were carried out with a Quantum Design SQUID magnetometer in the temperature range 1.9−300 K and under an applied magnetic field of 1 T in the high-temperature range and 250 G at low temperatures to avoid any problem of magnetic saturation. Diamagnetic corrections of the constituent atoms were estimated from Pascal's constants.

X-ray Data Collection and Structure Refinement. Crystals of dimensions $0.02 \times 0.12 \times 0.12$ (1), $0.11 \times 0.12 \times 0.16$ (2), $0.07 \times 0.11 \times 0.22$ (3), and $0.10 \times 0.11 \times 0.12$ mm^3 (4) were used for data collection on a Nonius Kappa CCD diffractometer using graphite-monochromated Mo Kα radiation (λ = 0.710 73 Å). A summary of the crystallographic data and structure refinement is given in Table 1. The index ranges of data collection were $-13 \leq h \leq 14$, $-19 \leq k \leq 21$, and $-45 \leq l \leq 45$ for 1, $-14 \leq h \leq 10$, $-17 \leq k \leq 20$, and $-43 \leq l \leq 45$ for 2, $-12 \leq h \leq 14$, $-20 \leq k \leq 20$, and $-42 \leq l \leq 44$ for 3, and $-14 \leq h \leq 11$, $-20 \leq k \leq 16$, and $-28 \leq l \leq 45$ for 4. Of the 6925 (1), 6858 (2), 6552 (3), and 5664 (4) measured independent reflections in the θ range 6.43−27.5° (1), 6.41−27.50° (2 and 3), and 6.40−27.50° (4), 5204 (1), 2945 (2), 4255 (3), and 3367 (4) have $I > 2\sigma(I)$. All the measured independent reflections were used in the analysis.

Table 1. Crystallographic Data for $(NBu_4)_2[\{Re^{IV}Cl_4(\mu\text{-ox})\}_2M^{II}(Him)_2]$ with M = Mn (**1**), Co (**2**), Ni (**3**), and Cu (**4**)

param	1	2	3	4
empirical formula	$C_{42}H_{80}Cl_8MnN_6O_8Re_2$	$C_{42}H_{80}Cl_8CoN_6O_8Re_2$	$C_{42}H_{80}Cl_8NiN_6O_8Re_2$	$C_{42}H_{80}Cl_8CuN_6O_8Re_2$
fw	1508.06	1512.05	1511.83	1516.66
space group	$C2/c$	$C2/c$	$C2/c$	$C2/c$
a, Å	10.9071(5)	10.960(3)	10.9599(6)	10.934(2)
b, Å	16.2650(5)	16.130(2)	16.1219(5)	16.016(2)
c, Å	35.2099(5)	34.961(2)	34.7243(7)	34.957(3)
β, deg	97.626(3)	96.89(2)	96.522(5)	97.20(2)
V, Å^3	6191.1(4)	6136(2)	6095.9(2)	6073.3(15)
Z	4	4	4	4
λ, Å	0.710 73	0.710 73	0.710 73	0.710 73
ρ_{calcd}, g cm^{-3}	1.618	1.637	1.647	1.659
T, K	293	293	293	293
μ(Mo Kα), cm^{-1}	0.4494	0.4599	0.4666	0.4723
R^a	0.0427	0.0991	0.0423	0.0480
$R_w{}^b$	0.0701	0.1181	0.0618	0.0671

^{a} $R = \Sigma(||F_o| - |F_c||/\Sigma|F_o|$. ^{b} $R_w = [[\Sigma(|F_o|^2 - |F_c|^2)^2/\Sigma|F_o|^2]^{1/2}$.

Table 2. Selected Bond Distances (Å) and Bond Angles (deg) for Compounds **1**–**4**^{a}

param	M = Mn (**1**)	M = Co (**2**)	M = Ni (**3**)	M = Cu (**4**)
Re(1)–O(1)	2.076(3)	2.052(9)	2.084(3)	2.084(4)
Re(1)–O(2)	2.078(3)	2.062(8)	2.079(3)	2.054(4)
Re(1)–Cl(1)	2.332(1)	2.330(4)	2.327(1)	2.330(2)
Re(1)–Cl(2)	2.304(1)	2.308(3)	2.304(1)	2.309(2)
Re(1)–Cl(3)	2.297(1)	2.304(3)	2.298(2)	2.303(2)
Re(1)–Cl(4)	2.332(2)	2.342(4)	2.336(2)	2.332(2)
M(1)–N(11)	2.154(4)	2.046(10)	2.017(4)	1.951(5)
M(1)–O(3)	2.244(3)	2.172(8)	2.134(3)	2.041(4)
M(1)–O(4)	2.247(3)	2.151(7)	2.096(3)	2.354(4)

param	M = Mn (**1**)	M = Co (**2**)	M = Ni (**3**)	M = Cu (**4**)
O(1)–Re(1)–O(2)	78.79(11)	79.5(3)	78.60(12)	78.8(2)
O(1)–Re(1)–Cl(1)	89.05(10)	90.0(3)	89.85(10)	89.29(13)
O(2)–Re(1)–Cl(1)	87.22(10)	87.0(3)	86.99(10)	87.10(14)
Cl(2)–Re(1)–Cl(1)	92.09(6)	92.42(13)	92.26(6)	91.90(7)
Cl(3)–Re(1)–Cl(1)	92.72(6)	92.71(14)	92.59(6)	92.58(8)
Cl(4)–Re(1)–Cl(1)	173.59(6)	173.83(15)	173.93(6)	173.96(8)
O(1)–Re(1)–Cl(2)	90.63(9)	90.6(2)	91.27(9)	91.47(12)
O(2)–Re(1)–Cl(2)	169.41(9)	170.0(2)	169.85(10)	170.24(13)
Cl(3)–Re(1)–Cl(2)	96.30(5)	96.16(14)	96.21(6)	96.24(7)
Cl(4)–Re(1)–Cl(2)	91.95(6)	91.63(15)	91.74(6)	91.60(8)
O(1)–Re(1)–Cl(3)	172.78(9)	172.6(2)	172.03(9)	172.00(12)
O(2)–Re(1)–Cl(3)	94.29(9)	93.8(2)	93.94(10)	93.50(14)
O(1)–Re(1)–Cl(4)	85.92(10)	85.3(3)	85.51(10)	85.70(14)
O(2)–Re(1)–Cl(4)	87.89(11)	88.2(3)	88.26(10)	88.61(14)
Cl(3)–Re(1)–Cl(4)	91.79(6)	91.48(15)	91.50(6)	91.93(8)

| param	M = Mn (**1**)	M = Co (**2**)	M = Ni (**3**)	M = Cu (**4**)
N(11)–M(1)–N(11a)	94.0(2)	95.6(6)	92.7(2)	93.5(3)
N(11)–M(1)–O(3a)	162.41(13)	167.4(4)	170.41(14)	165.8(2)
N(11)–M(1)–O(3)	91.85(15)	91.0(4)	91.19(14)	91.3(2)
O(3a)–M(1)–O(3)	87.47(18)	84.6(5)	86.4(2)	87.4(2)
N(11)–M(1)–O(4a)	88.12(13)	90.5(4)	91.02(14)	89.2(2)
O(3)–M(1)–O(4a)	93.58(12)	92.5(3)	91.03(12)	92.6(2)
N(11)–M(1)–O(4)	103.17(14)	98.2(4)	97.67(14)	100.8(2)
O(3)–M(1)–O(4)	74.39(11)	77.9(3)	79.76(12)	76.7(2)
O(4a)–M(1)–O(4)	163.55(17)	167.1(4)	167.4(2)	165.4(2)

^{a} Symmetry code: (a) $-x + 1$, y, $-z + 1/2$.

The structures of **1**–**4** were solved by direct methods and refined with full-matrix least-squares technique on F^2 using the SHELXL-97[10] program included in the WINGX[11] package. All non-hydrogen atoms were refined anisotropically. Some of the tetra-*n*-butylammonium carbon atoms are thermally disordered. The hydrogen atoms were set in calculated positions and refined with isotropic temperature factors. Full-matrix least-squares refinement was performed. The values of the discrepancy indices R/R_w for all data were 0.0677/0.0755 (**1**), 0.2503/01459 (**2**), 0.0883/0.0707 (**3**), and 0.1113/0.0841 (**4**) [those listed in Table 1 correspond to the data with $I > 2\sigma(I)$]. The final Fourier-difference map showed maximum and minimum height peaks of 1.398 and -0.579 e Å^{-3} for **1**, 1.304 and -0.944 e Å^{-3} for **2**, 0.634 and -0.451 e Å^{-3} for **3**, and 0.787 and -0.495 e Å^{-3} for **4**. The values of the number of reflections $[I > 2\sigma(I)]$/number of parameters are 17.2 (**1**), 9.7 (**2**), 14.0 (**3**), and 11.1 (**4**), whereas those of the goodness-of-fit are 1.080 (**1**),

(10) Sheldrick, G. M. *SHELX97, Programs for Crystal Structure Analysis*, release 97-2; Institüt für Anorganische Chemie der Universität: Tammanstrasse 4, D-3400 Göttingen, Germany, 1998.
(11) Farrugia, L. J. *J. Appl. Crystallogr.* **1999**, *32*, 837.
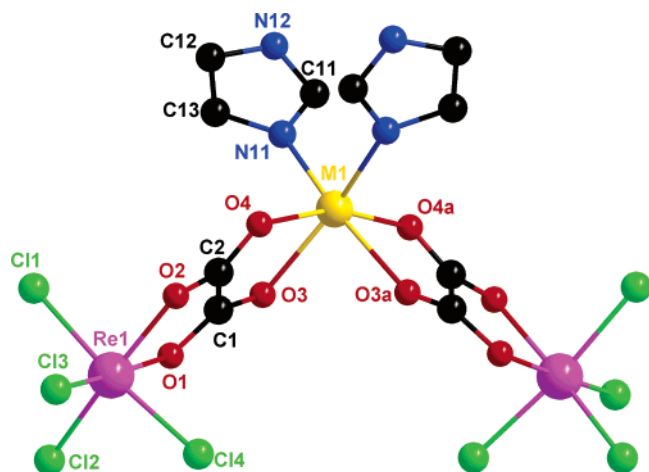
Figure 1. Perspective drawing of the heterotrinuclear unit of **1**−**4** with M = Mn (**1**), Co (**2**), Ni (**3**), and Cu (**4**) showing the atom numbering. Hydrogen atoms have been omitted for clarity.

1.047 (**2**), 1.019 (**3**), and 1.016 (**4**). The final geometrical calculations and graphical manipulations were carried out with the PARST97[12] and CRYSTALMAKER[13] programs. Selected bond distances and angles for **1**−**4** are listed in Table 2.

Crystallographic data (excluding structure factors) for the structures reported in this paper have been deposited at the Cambridge Data center as supplementary publications nos. CCDC 625213 (**1**), 625214 (**2**), 625215 (**3**), and 625216 (**4**) Copies of the data can be obtained free of charge on application to CCDC, 12 Union Road, Cambridge CB21EZ, U.K. (fax (+44) 1223−336-033; e-mail deposit@ccdc.cam.ac.uk).

Results and Discusion

Description of the Structures of $(NBu_4)_2[\{ReCl_4(\mu\text{-}ox)\}_2M(Him)_2]$ [M = Mn (1), Co (2), Ni (3), and Cu (4)]. **1**−**4** are isostructural compounds whose structure is made up of $[\{ReCl_4(ox)\}_2M(Him)_2]^{2-}$ trinuclear anions [M = Mn (**1**), Co (**2**), Ni (**3**), and Cu (**4**)] and tetra-*n*-butylammonium cations which are held together by electrostatic forces, hydrogen bonds, and van der Waals interactions (see below). A perspective drawing of the structure of the anionic unit along with the atom numbering is depicted in Figure 1. Each $[\{ReCl_4(ox)\}_2M(Him)_2]^{2-}$ unit contains two peripheral rhenium atoms and one central M atom which are interconnected through two bis-bidentate oxalate ligands.

Each rhenium atom is surrounded by two oxalate oxygen and four chloride anions building a distorted octahedral environment. The short bite of the oxalate is the main cause of the distortion, the value of the angle subtended by this ligand at the rhenium atom [O(1)−Re(1)−O(2)] varying in the range 78.60(12) (**3**) to 79.5(3)° (**2**). No significant differences were found in the Re−Cl [values covering the range 2.2969(13)−2.342(4) Å] and Re−O [maximum and minimum values being 2.084(3) and 2.052(9) Å, respectively] bond distances in this family. Bond lengths and angles within the [ReCl_4(ox)] fragment are in agreement with those found for this unit in previous reports.[2a,b,6,7] The best equatorial

(12) Nardelli, M. *J. Appl. Crystallogr.* **1995**, *28*, 659.
(13) *CrystalMaker*, 4.2.1; CrystalMaker Software: Bicester, Oxfordshire X26 3TA, U.K.

plane around the rhenium atom is defined by the O(1)O(2)-Cl(2)Cl(3) set of atoms, the largest deviation from planarity being 0.036(3) (**1**), 0.056(9) (**2**), 0.050(3) (**3**), and 0.0515-(5) (**4**) Å at O(2). The Re atom lies in this plane in the four compounds, the maximum deviation being 0.0270(6) Å for compound **2**. The values of the dihedral angle between the equatorial plane and that of the oxalate group are 4.78(7) (**1**), 5.6(2) (**2**), 5.51(7) (**3**), and 4.79(8)° (**4**).

The M atoms are also six-coordinated with four oxalate oxygen atoms from two [ReCl_4(ox)]^{2-} units and two imidazole nitrogen atoms from two terminal imidazole ligands in cis position building somewhat distorted octahedral surroundings. As observed at the Re atom, the main source of distortion of the ideal octahedral geometry at the M atom is due to the reduced bite of the oxalate [the values of the O(3)−M(1)−O(4) bond vary in the range 74.39(11) (**1**) to 79.76(12)° (**3**)]. The M atom lies on a 2-fold axis. The values of the imidazole to M bond distances decreases when going from the manganese(II) [2.154(4) Å] to the copper(II) [1.951-(5) Å] in agreement with the trend exhibited by the values of the ionic radii of the first row metal ions. The values of the M−N(imidazole) bonds in **1**−**4** are very close to those observed in other imidazole-containing M(II) complexes.[14] Bond lengths and angles within the imidazole ring are in agreement with the parameters reported for the structure of free imidazole at 150 °C.[15] The oxalate ligand of the [ReCl_4(ox)] unit is coordinated to the M atom in symmetrical (**1**−**3**) and asymmetrical (**4**) chelating modes, the M−O bonds being longer [2.244(3) and 2.247(3) Å (**1**), 2.172(8) and 2.151(7) Å (**2**), 2.134(3) and 2.096(3) Å (**3**), and 2.041(4) and 2.353(4) Å (**4**)] than those of the M−N(imidazole). The values of the M−O(ox) bond distances in **1**−**4** are close to those observed for other oxalate-bridged compounds.[6,7,16] Both the oxalate and Him ligands are planar. The values of the dihedral angles of the ox/ox, Him/Him, and ox/Him pairs vary in the ranges 83.80(10) (**4**) to 86.24(8)° (**1**), 73.9(2) (**1**) to 78.1(3)° (**4**), and 85.5(2) (**4**) to 88.8(2)° (**1**), respectively. The values of the Re···M separation across the bridging oxalate are 5.611(1) (**1**), 5.505(2) (**2**), 5.451(1) (**3**), and 5.536-(1) Å (**4**).

The shortest intermolecular chloro···chloro distances are 5.794(2) (**1**), 5.671(6) (**2**), 5.646(2) (**3**), and 5.651(3) Å (**4**), values that are beyond the sum of the van der Waals radii. The heterometallic trinuclear units of **1**−**4** are interconnected through weak N−H···O hydrogen bonds [N(12)···O(1b) =

(14) (a) Lehnert, R.; Seel, F. *Z. Anorg. Allg. Chem.* **1980**, *464*, 187. (b) Horrocks, W. D.; Ishley, J. N.; Whittle, R. R. *Inorg. Chem.* **1982**, *21*, 3265. (c) Horrocks, W. D.; Ishley, J. N.; Whittle, R. R. *Inorg. Chem.* **1982**, *21*, 3270. (d) Yu, J. H.; Xu, J. Q.; Zhang, L. J.; Lu, J.; Zhang, X.; Bie, H. Y. *J. Mol. Struct.* **2005**, *743*, 243. (e) Dvorkin, A. A.; Simonov, Y. A.; Sliva, T. Yu, Lampeka, R. D.; Mazus, M. D.; Skopenko, V. V.; Malinovskii, T. I. *Russ. J. Inorg. Chem.* **1989**, *34*, 2582. (f) Zhang, Y.; Li, J.; Lin, W.; Liu, S.; Huang, J. *J. Crystallogr. Spectrosc. Res.* **1992**, *22*, 433. (g) Masciocchi, N.; Ardizzoia, G. A.; LaMonica, G.; Maspero, A.; Galli, S.; Sironi, A. *Inorg. Chem.* **2001**, *40*, 6983. (h) Glowiak, T.; Wnek, I. *Acta Crystallogr., Sect. C: Cryst. Sect. Commun.* **1985**, *41*, 324. (i) Huo, L. H.; Gao, S.; Zhao, H. Ng, S. W. *Acta Crystallogr., Sect. E: Struct. Rep. Online* **2004**, *60*, m1747. (j) Lin, J. L.; Zheng, Y. Q. *Z. Krystallogr.-New Cryst. Struct.* **2004**, *219*, 431. (k) Rahaman, S. H.; Chowdhury, H.; Bose, D.; Mostafa, G.; Fun, H. F.; Ghosh, B. K. *Inorg. Chem. Commun.* **2005**, *8*, 1041.
(15) Martínez-Carrera, S. *Acta Crystallogr.* **1966**, *20*, 783.
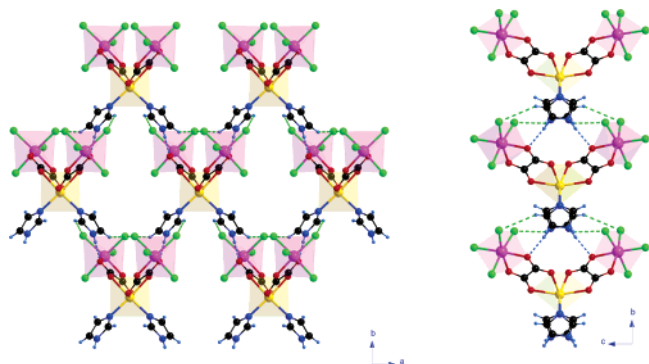
Figure 2. View along the *c*- (left) and *a*-axes (right) of a fragment of the sheet formed by the [{ReCl$_4$(μ-ox)}$_2$M(Him)$_2$] unit through C−H•••Cl and N−H•••O interactions (broken lines). Pink, yellow, red, green, and blue colors refer to Re, M, O, Cl, and imidazole nitrogen atoms, respectively.

2.899(8) (**1**), 2.938(2) (**2**), 2.929(6) (**3**), and 2.940(9) Å (**4**) Å; (b) = −*x* + 1/2, *y* − 1/2, −*z* + 1/2] and C−H•••Cl type interactions [C(12)•••Cl(4b) = 3.70(1) (**1**), 3.65(2) (**2**), 3.667-(8) (**3**), and 3.630(12) Å (**4**); C(11)•••Cl(2c) = 3.830(7) (**1**), 3.788(15) (**2**), 3.774(6) (**3**), and 3.651(7) Å (**4**); C(21)•••Cl-(2d) = 3.651(5) (**1**), 3.638(14) (**2**), 3.659(5) (**3**), and 3.657-(7) Å (**4**); C(22)•••Cl(3) = 3.800(5) (**1**), 3.814(14) (**2**), 3.805(5) (**3**), and 3.887(7) Å (**4**); C(33)•••Cl(1e) = 3.830(6) (**1**), 3.797(14) (**2**), 3.821(6) (**3**), and 3.797(8) Å (**4**); (c) = *x* − 1/ 2, *y* − 1/2, *z*; (d) = *x* + 1/2, *y* − 1/2, *z*; (e) = *x* + 1, *y*, *z*] affording anionic layers which grow in the *ab* plane (Figure 2) and that are separated from each other by layers of tetra-*n*-butyl ammonium cations. The bulky organic cation exhibits its usual tetrahedral shape with bond lengths and angles in agreement with those reported for this entity in previous reports.[17] Interestingly, each NBu$_4^+$ cation interacts with three chloro atoms from three [ReCl$_4$(ox)] units via weak C−H•••Cl type interactions as shown in Figure S1.

Magnetic Properties of 1−4. In this section, prior to the description and corresponding analysis of the magnetic data of **1−4** and having in mind the presence of the [ReCl$_4$(ox)]$^{2-}$ unit as a ligand in them, we will remind of first the magnetic

(16) (a) Julve, M.; Verdaguer, M.; Gleizes, A.; Philoche-Levisalles, M.; Kahn, O. *Inorg. Chem.* **1984**, *23*, 3808. (b) Battaglia, L. P.; Bianchi, A.; Corradi, A. B.; García-España, E.; Micheloni, M.; Julve, M. *Inorg. Chem.* **1988**, *27*, 4174. (c) Oshio, H.; Nagashima, U. *Inorg. Chem.* **1992**, *31*, 3295. (d) De Munno, G.; Julve, M.; Nicolò, F.; Lloret, F.; Faus, J.; Ruiz, R.; Sinn, E. *Angew. Chem., Int. Ed. Engl.* **1993**, *32*, 613. (e) Ohba, M.; Tamaki, H.; Matsumoto, N.; Okawa, H. *Inorg. Chem.* **1993**, *32*, 5385. (f) De Munno, G.; Ruiz, R.; Lloret, F.; Faus, J.; Sessoli, R.; Julve, M. *Inorg. Chem.* **1995**, *34*, 408. (g) Glerup, J.; Goodson, P. A.; Hodgson, D. J.; Michelsen, K. *Inorg. Chem.* **1995**, *34*, 6255. (h) Román, P.; Guzmán-Miralles, C.; Luque, A.; Beitia, J. I.; Cano, J.; Lloret, F.; Julve, M.; Alvarez, S. *Inorg. Chem.* **1996**, *35*, 3741. (i) Akhriff, Y.; Server-Carrión, J.; Sancho, A.; García-Lozano, J.; Escrivá, E.; Folgado, J. V.; Soto, L. *Inorg. Chem.* **1999**, *38*, 1174. (j) Castillo, O.; Luque, A.; Román, P.; Lloret, F.; Julve, M. *Inorg. Chem.* **2001**, *40*, 5526. (j) García-Terán, J. P.; Castillo, O.; Luque, A.; García-Couceiro, U.; Román, P.; Lloret, F. *Inorg. Chem.* **2004**, *43*, 5761.

(17) (a) Atovmyan, L. O.; Shilov, G. V.; Lyobovskaya, R. N.; Zhilyaeva, E. I.; Ovanesyan, N. S.; Pirumova, S. I.; Gusakovskaya, I. G. *JETP Lett.* **1993**, *58*, 766. (b) Mathonière, C.; Nuttall, C. J.; Carling, S. G.; Day, P. *Inorg. Chem.* **1996**, *35*, 1201. (c) Péllaux, R.; Schmalle, H. W.; Huber, R.; Fischer, P.; Hauss, T.; Ouladdiaf, B.; Decurtins, S. *Inorg. Chem.* **1997**, *36*, 2301. (d) Masters, V. M.; Sharrad, C. A.; Bernhardt, P. V.; Gahan, L. R.; Moubaraki, B.; Murray, K. S. *J. Chem. Soc., Dalton Trans.* **1998**, 413.
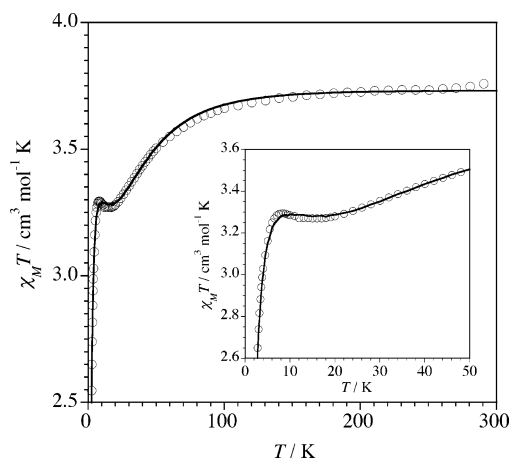
Figure 3. Thermal dependence of $\chi_M T$ for **4**: (○) experimental data; (−) best-fit curve (see text). The inset shows details of the low-temperature range.
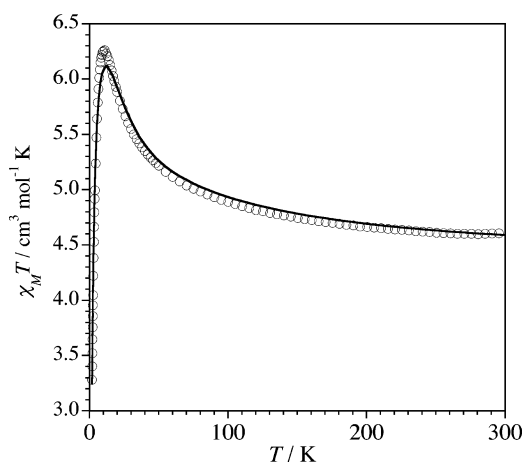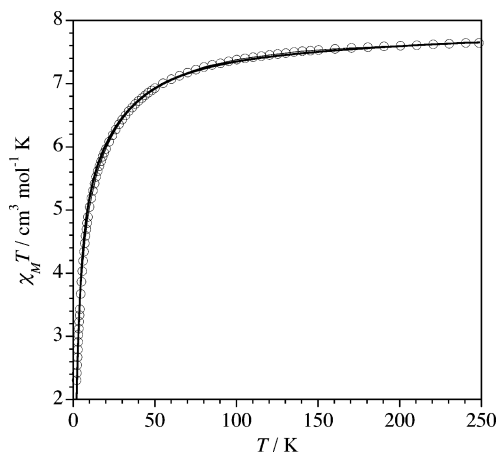

Figure 4. Thermal dependence of $\chi_M T$ for **3**: (○) experimental data; (−) best-fit curve (see text).
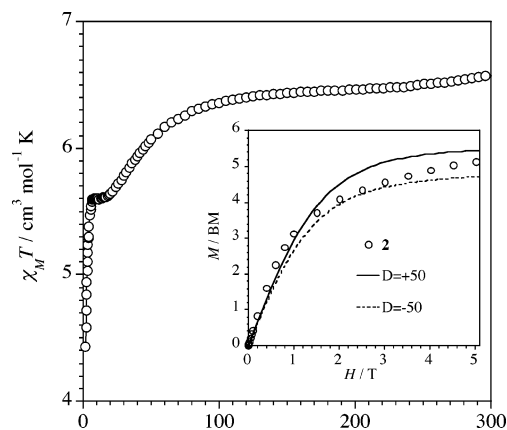
Figure 5. Thermal dependence of $\chi_M T$ for **2**. The inset shows the magnetization versus *H* plot for **2** at 2.0 K. The open circles are the experimental data; the lines correspond to one Co(II) (S_{eff} = 1/2 and g_{Co} = 4.3) and two Re(IV) (S_{Re} = 3/2, g_{Re} = 1.85, and D_{Re} = ±50 cm^{-1}) ions magnetically isolated.

behavior of such a Re(IV) unit when it is magnetically isolated. Then, we will describe and analyze the magnetic properties of **1−4** (see Figures 3−6 where χ_M is the magnetic susceptibility/Re$^{IV}_2$M^{II} unit) by following the increasing number of unpaired electrons on the M^{II} cation for pedagogical reasons.

Figure 6. Thermal dependence of $\chi_M T$ for **1**: (○) experimental data; (—) best-fit curve (see text).

Table 3. Best-Fit Parameters for **1**, **3**, and **4**

param	1	3	4
J, cm^{-1}	−0.35	+14.2	+7.7
D_{Re}, cm^{-1}	35.7	63.5	45.8
g_{Re}	1.90	1.82	1.86
g_M	2.00	2.14	2.11
Θ, K			−1.6^a
R^b	1.2×10^{-5}	2.5×10^{-4}	1.6×10^{-5}

^{a} A Curie−Weiss term accounting for the intermolecular interactions. ^{b} R is the agreement factor defined as $\Sigma_i[(\chi_M T)\text{obs}(i) - (\chi_M T)\text{calc}(i)]^2/\Sigma_i[(\chi_M T)\text{obs}(i)]^2$.

Concerning the first point, the value of $\chi_M T$ at room temperature for such a magnetically isolated $[Re^{IV}Cl_4(ox)]^{2-}$ unit is ca. 1.60 cm^3 mol^{-1} K (per rhenium atom) with $S_{Re} = 3/2$ and $g_{Re} = 1.8-1.9$.[2a] Upon cooling, and in the lack of intermolecular interactions, this value decreases because of zero field splitting effects ($2D_{Re}$) resulting from the combined action of the second-order spin−orbit interaction and the tetragonal crystal field of the six-coordinated Re(IV) [$2D_{Re}$ is the energy gap between the $M_S = \pm3/2$ and $M_S = \pm1/2$ Kramers doublets]. At low temperatures where $kT \ll |2D_{Re}|$, this unit can be regarded as an Ising-spin-1/2 system[18] with a $\chi_{av}T$ value of ca. 1.0 cm^3 mol^{-1} K (χ_{av} being the average powder susceptibility with $g = g_{\parallel} = g_{\perp}$).

The value of $\chi_M T$ for **4** at room temperature is 3.76 cm^3 mol^{-1} K (Figure 3), as expected for one Cu(II) ($\chi_M T = 0.41$ cm^3 mol^{-1} K with $S_{Cu} = 1/2$ and $g = 2.1$) and two Re(IV) ions magnetically isolated ($\chi_M T =$ ca. $2 \times 1.6 + 0.4 = 3.6$ cm^3 mol^{-1} K; see above). This value decreases smoothly upon cooling, exhibits a minimum at $T = 16$ K with $\chi_M T = 3.27$ cm^3 mol^{-1} K, then increases slightly to 3.30 cm^3 mol^{-1} K at 8.0 K and further decreases sharply to 2.03 cm^3 mol^{-1} K at 1.9 K. The fact that the value at the minimum of $\chi_M T$ is well above that calculated for one Cu-(II) and two Re(IV) ions with zero field splitting which are magnetically isolated ($\chi_M T =$ ca. $2 \times 1.0 + 0.4 = 2.4$ cm^3 mol^{-1} K) reveals that an intramolecular ferromagnetic interaction is involved in **4**. This interaction is obscured by the decrease of $\chi_M T$ in the intermediate and low-temperature range which is most likely due to the combination of zero field splitting effects and intermolecular (very low temperatures) interactions. Having into account the trinuclear structure of **4** and the above magnetic considerations, we have analyzed its magnetic data through the Hamiltonian of eq 1,

$$H = -J(S_{Re1} \cdot S_M + S_{Re2} \cdot S_M) + D_{Re1}[S_{zRe1}^2 - 5/4] + D_{Re2}[S_{zRe2}^2 - 5/4] + D_M[S_{zM}^2 - n(n+2)/12] + \beta(S_{Re1}g_{Re1} + S_{Re2}g_{Re2} + S_Mg_M) \cdot H \quad (1)$$

where J is the exchange coupling parameter between each peripheral Re(IV) and the central M(II) local spins [M = Cu (**4**)], n is the number of unpaired electrons on the M(II) center ($n = 1$ for **4**), and D_M is the zero field splitting of the M(II) ions (it is strictly zero for M = Cu). The last term in the eq 1 accounts for the Zeeman effects of the three metal ions. To reduce the large number of variable parameters to avoid overparametrization, we have assumed that $g = g_{\parallel} = g_{\perp}$ for the Re(IV) and Cu(II) ions. Least-squares fit of the magnetic data of **4** through eq 1 leads to the parameters listed in Table 3. As one can see in Figure 3, the calculated curve matches very well the experimental data.

$\chi_M T$ at room temperature for **3** is 4.60 cm^3 mol^{-1} K (Figure 4), a value which is as expected for a Ni(II) ion ($S_{Ni} = 1$) and two Re(IV) centers ($S_{Re} = 3/2$) magnetically noninteracting. It increases very slowly upon cooling, reaching a maximum value of 6.26 cm^3 mol^{-1} K at 11 K and decreases steeply at lower temperatures. These features reveal an intramolecular ferromagnetic coupling in **3**, the local anisotropy of the metal ions (ZFS effects), and/or weak intermolecular antiferromagnetic interactions accounting for the decrease of $\chi_M T$ in the low-temperature range. The magnetic data of **3** were analyzed through the Hamiltonian of eq 1 but replacing M by Ni (with $n = 2$ and D_{Ni} representing the energy gap between the sublevels $M_S = 0$ and $M_S = \pm1$). As previously done for **4**, we have assumed that $g = g_{\parallel} = g_{\perp}$ for the Re(IV) and Ni(II) ions in **3**. The best-fit parameters are listed in Table 3. The computed curve reproduces reasonably well the experimental magnetic data.

The value of $\chi_M T$ for **2** at room temperature is 6.50 cm^3 mol^{-1} K (Figure 5). This value is consistent with the presence of a high-spin Co(II) ion ($S_{Co} = 3/2$ with unquenched orbital momentum) and two Re(IV) cations magnetically noninteracting. It decreases smoothly upon cooling to reach a quasi plateau in the temperature range 20−9.0 K ($\chi_M T = 5.60$ cm^3 mol^{-1} K) and again decreases at lower temperature to reach a value of 4.42 cm^3 mol^{-1} K at 1.9 K. These features are interpreted as follows: the spin−orbit coupling effects of the high-spin Co(II) ion (depopulation of the higher energy Kramers doublets) and the zero field splitting of the two Re-(IV) ions account for the decrease of $\chi_M T$ in the high-temperature range whereas the quasi plateau would be due to the competition between the previous effects and an intramolecular ferromagnetic interaction between the Re(IV) and the Co(II) ions. The occurrence of an intramolecular ferromagnetic interaction in **2** is supported by the fact that the $\chi_M T$ value at 1.9 K is well above the calculated one for a magnetically noninteracting Re(IV)−Co(II)−Re(IV) three

(18) Ising, E. *Z. Phys.* **1925**, *31*, 253.

spin set at such low temperature ($\chi_M T$ ca. 3.65 cm^3 mo^{-1} K) [one must take into account that $\chi_M T$ for a magnetically isolated Re(IV) center tends to a finite value close to 1.0 cm^3 mol^{-1} K at 1.9 K (see above) and that, at $T <$ 30 K, the Co(II) ion has an S_{eff} = 1/2 with a g value of ca. 4.2].[19] If one thinks of the analysis of the magnetic data of **2**, it must be noted that the above spin Hamiltonian is applicable only to metal ions with nondegenerate ground terms in an octahedral environment, a condition which is not satisfied by the six-coordinated Co(II). As this cation has a $^4T_{1g}$ ground term, it is split into a sextet, a quartet, and a Kramers doublet by spin−orbit coupling.[19,20] In addition, the axially distorted six-coordinated Co(II) in **2** splits the T term giving a nondegenerate ground term. Consequently, the spin Hamiltonian for the case of **2** becomes very complex. This fact together with the strong correlation that we observed among the large number of parameters involved did not provide a reliable set of parameters in the fit of the magnetic data of this complex.

The value of $\chi_M T$ for **1** at room temperature is 7.60 cm^3 mol^{-1} K (Figure 6). This value which is as expected for the set of one Mn(II) ($\chi_M T$ = 4.375 cm^3 mol^{-1} K with S_{Mn} = 5/2 and g_{Mn} = 2.0) and two Re(IV) ions (see above) magnetically isolated. Upon cooling, it decreases first slowly and then faster, reaching a value of 2.30 cm^3 mol^{-1} K at 1.9 K. No maximum of the magnetic susceptibility is observed for **1** in the temperature range explored. Most of the variation of $\chi_M T$ with T is due to the zero field splitting of Re(IV) and certainly a weak antiferromagnetic coupling between the Re(IV) ions and the Mn(II) center through the oxalato bridge. This antiferromagnetic interaction between Re(IV) and Mn-(II) is supported by the fact that the value of $\chi_M T$ at low temperature (ca. 2.3 cm^3 mol^{-1} K) is well below the expected one for the three magnetically isolated cations ($\chi_M T$ = ca. 2 × 1 + 4.4 = 6.4 cm^3 mol^{-1} K) in contrast to **2**−**4**. The analysis of the magnetic data of **1** through the Hamiltonian of eq 1, where M is replaced by Mn with n = 5, D_{Mn} = 0, and under the assumption that $g = g_{\parallel} = g_{\perp}$ for the Re(IV) and Mn(II) ions, leads to the set of best-fit parameters which are given in Table 3. One can see in Figure 6 that the calculated curve for **1** reproduces well the magnetic data.

The magnetization versus H plots for complexes **1**−**4** were performed at 2.0 K. Those for **1**, **3**, and **4** are shown in Figure 7. The experimental data therein can be reproduced by using the parameters listed in Table 3, indicating the good agreement existing between the magnetization and magnetic susceptibility measurements. The corresponding M vs H plot for complex **2** is shown in the inset of Figure 5. For comparative purposes, two theoretical curves corresponding
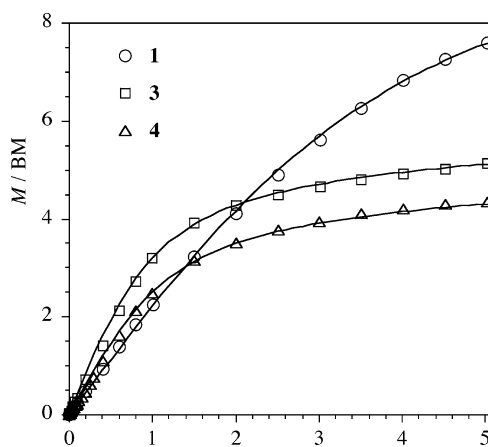
Figure 7. Magnetization versus H plot for **1**, **3**, and **4** at 2.0 K. The symbols are the experimental data; the solid lines are the theoretical curves using the parameters of Table 3.

to one Co(II) (S_{eff} = 1/2 and g_{Co} = 4.3)[21] and two Re(IV) (S_{Re} = 3/ 2, g_{Re} = 1.85, and D_{Re} = ±50 cm^{-1}) ions magnetically noninteracting are included. One can see how the experimental data increase faster than the calculated plots supporting the occurrence of a ferromagnetic coupling.

The occurrence of intramolecular antiferro- (**1**) and ferromagnetic (**2**−**4**) interactions has additional support on previous findings concerning the oxalato-bridged heterobimetallic complexes [ReCl$_4$(μ-ox)M(dmphen)$_2$]·MeCN, where intramolecular antiferro- (J_{ReMn} = −0.2 cm^{-1}) and ferromagnetic (J_{ReCo} = +10.4 cm^{-1} and J_{ReNi} = +11.8 cm^{-1}) interactions were observed.[6,22] Very recently, the tetranuclear species (NBu$_4$)$_4$[Ni{ReCl$_4$(μ-ox)}$_3$], where a central Ni(II) ion is tris-chelated by three [ReCl$_4$(μ-ox)]$^{2-}$ ligands, provided the second example of ferromagnetic coupling between Ni-(II) and Re(IV) through bis-bidentate oxalate (J_{ReNi} = + 16.3 cm^{-1}).[7] For the case of **4**, although a very weak antiferromagnetic interaction (J_{ReCu} = −0.90 cm^{-1}) was observed through bis-bidentate oxalate in the complex [ReCl$_4$(μ-ox)-Cu(phen)$_2$]·MeCN,[2b] the different copper to oxalate oxygen bonding pattern [two long Cu−O(ox) bonds of 2.32(2) and 2.41(2) Å in this latter compound versus one short and one long Cu−O(ox) bonds of 2.041(4) and 2.353(4) Å in **4**] would account for the different nature of the magnetic coupling in them.

The nature of the magnetic interaction in **1**−**4** can be understood through orbital symmetry considerations. Assuming an octahedral symmetry for the metal ions, the three unpaired electrons on the Re(IV) ion are defined by t_{2g} type orbitals whereas in the Mn(II), Co(II), Ni(II), and Cu(II) ions the electronic configurations are $t_{2g}^3 e_g^2$, $t_{2g}^5 e_g^2$, $t_{2g}^6 e_g^2$, and $t_{2g}^6 e_g^3$, respectively. Consequently, in the case of the

(19) (a) Mishra, V.; Lloret, F.; Mukherjee, R. *Inorg. Chim. Acta* **2006**, *359*, 4053. (b) Maspoch, D.; Domingo, N.; Ruiz-Molina, D.; Wurst, K.; Hernández, J. M.; Vaughan, G.; Rovira, C.; Lloret, F.; Tejada, J.; Veciana, J. *Chem. Commun.* **2005**, 5035. (c) Herrera, J. M.; Bleuzen, A.; Dromzée, Y.; Julve, M.; Lloret, F.; Verdaguer, M. *Inorg. Chem.* **2003**, *42*, 7052. (d) Colacio, E.; Lloret, F.; Ben-Maimoun, I.; Kivekas, R.; Sillanpaa, R.; Suárez-Varela, J. *Inorg. Chem.* **2003**, *42*, 2720.

(20) Figgis, B. N.; Gerloch, M.; Lewis, J.; Mabbs, F. E.; Webb, G. A. *J. Chem. Soc. A* **1968**, 2086.

(21) (a) Herrera, J. M.; Bleuzen, A.; Dromzée, Y.; Julve, M.; Lloret, F.; Verdaguer, M. *Inorg. Chem.*, **2003**, *42*, 7052. (b) Rodriguez, A.; Sakiyama, H.; Masciocchi, N.; Galli, S.; Galez, N.; Lloret, F.; Colacio, E. *Inorg. Chem.* **2005**, *44*, 8399. (c) Mishra, V.; Lloret, F.; Mukherjee, R. *Inorg. Chim. Acta* **2006**, *359*, 4053.

(22) The real values of the magnetic coupling for the heterobimetallic Re^{IV}−M^{II} (M = Mn, Fe, Co, and Ni) that we reported in ref 6 have to be multiplied by two because although we specified that the spin Hamiltonian used was $H = -JS_A \cdot S_B$, it was indeed $H = -2JS_A \cdot S_B$. We check this error by a careful inspection of the theoretical expression that we used to carry out the fits of the corresponding magnetic data.

compounds **3** and **4**, the orthogonality between the t_{2g} [Re-(IV)] and e_g [Ni(II) and Cu(II)] type magnetic orbitals accounts for the ferromagnetic coupling observed in them. When one goes from **3** to **2**, although three antiferromagnetic terms (those issuing from the half filled t_{2g} orbital) have to be added, the magnetic data show that the ferromagnetic terms are still dominant. Finally, the presence of three half-filled t_{2g} orbitals on the Mn(II) ion in **1** increases the antiferromagnetic contributions leading to a quasi compensation between the ferro- and antiferromagnetic contributions and a very small and negative J value results.

Finally, we finish this work with a brief comment concerning the magnitude of the ferromagnetic coupling for this family of compounds, which is related to the diffuse character of the magnetic orbitals involved. In this respect, it deserves to be noted that the ferromagnetic coupling between Cr(III) and Ni(II) through oxalate in the tetranuclear compound [Cr(μ-ox)$_3$Ni$_3$(Me$_6$[14]ane-N$_4$)$_3$](ClO$_4$)$_3$ (Me$_6$[14]-ane-N$_4$ = ($\pm$)-5,7,7,12,14,14,-hexamethyl-1,4,8,11-tetraaza-cyclotetradecane) is $J = +5.3$ cm^{-1}.[9] This value is close to half of those observed in the previous family containing Re-(IV) (a 5d^3 system) instead of Cr(III) (a 3d^3 system). The greater diffuseness of the 5d versus 3d orbitals accounts for the larger ferromagnetic coupling in the Re(IV)−Ni(IV) pair when compared to the Cr(III)−Ni(II) unit. This result shows the interest in the magnetic study of mixed 5d/3d systems which are scarcely investigated when compared to the great number of studies being currently done with 3d/3d ones.

Supporting Information Available: A view of the C−H···Cl interactions concerning the NBu$_4^+$ group (Figure S1). This material is available free of charge via the Internet at htpp://pubs.acs.org.

IC0622095